Proceedings of the 2004 Performance Metics for Intelligent Systems (PerMIS) Workshop, Gaithersburg, MD, August 24 - 26, 2004.

Performance Evaluation of Temporal Range Registration for Unmanned Vehicle Navigation

R. Madhavan and E. Messina
Intelligent Systems Division
National Institute of Standards and Technology
Gaithersburg, MD 20899-8230.
Tel: (301) 975-2865 Fax: (301) 990-9688
Email: {raj.madhavan, elena.messina}@nist.gov

ABSTRACT— In this paper, we evaluate the performance of an iterative registration algorithm for position estimation of Unmanned Ground Vehicles (UGVs) operating in unstructured environments. Field data obtained from trials on UGVs traversing undulating outdoor terrain is used to quantify the performance of the algorithm in producing continual position estimates. These estimates are then compared with those provided by ground truth to facilitate the performance evaluation of the algorithm. Additionally, we propose performance measures for assessing the quality of correspondences. These measures, collectively, provide an indication of the quality of the correspondences thus making the registration algorithm more robust to outliers as spurious matches are not used in computing the incremental transformation.

Keywords:

UGV, range images, registration, uncertainty, performance measures.

1. INTRODUCTION

Active range sensing has become an integral part of any unmanned vehicle navigation system due its ability to produce unambiguous, direct, robust, and precise images consisting of range pixels. This is in direct contrast to passive sensing where the inference of range largely remains computationally intensive and not robust enough for use in natural outdoor environments. Depending on the speed of the vehicle, operating environment, and data rate, such range images acquired from a moving platform need to be registered to make efficient use of information contained in them for various navigation tasks including map-building, localization, obstacle avoidance, and control.

Iconic methods that attempt to minimize the discrepancies between sensed data and a model of the environment have been utilized for range registration. The attraction of these methods lies in the fact that the matching works directly on data points. Because the search is confined to small perturbations of the range images, it is computationally efficient. For example, Kanade et al. [3] compared elevation maps obtained from 3D range images to determine vehicle location. A similar iconic approach has also been adopted by Shaffer [10] but it does not take into account the uncertainty associated with the observation data.

We have developed a temporal iterative algorithm for registering range images obtained from unmanned vehicles. Formally, the process of registration is defined as follows: Given two sets of range images (model set: $\mathbf{M}$ and data set: $\mathbf{D}$), find a transformation (rotation and translation) which when applied to $\mathbf{D}$ minimizes a distance measure between the two point sets. Despite the apparent simplicity of the problem, to register range images from unmanned vehicles traversing unstructured environments, the terrain of travel, sensor noise and determination of accurate correspondences make it quite challenging.

The registration algorithm is a modified variant of the well-known Iterative Closest Point (ICP) algorithm [1]. At each iteration, the algorithm determines the closest match for each point and updates the estimated position based on a least-squares metric with some modifications to increase robustness. The modified algorithm has been shown to be robust to outliers and false matches during the registration of 3D range images obtained from a scanning LADAR rangefinder on an Unmanned Ground Vehicle (UGV) and also towards registering LADAR images from the UGV with those from an Unmanned Aerial Vehicle (UAV) that flies over the terrain being traversed [9]. For completeness, the temporal iterative registration algorithm is summarized in Section 2.

In this paper, we evaluate the performance of the registration algorithm for position estimation of UGVs operating in unstructured environments. Field data obtained from two trials on UGVs traversing undulating outdoor terrain is used to quantify the performance of the algorithm in producing continual position estimates. Using the data obtained from the first trial, the iterative registration algorithm aids the position estimation process whenever Global Positioning System (GPS) estimates are unavailable or are below required accuracy bounds. In the second trial, ICP is combined with a post-correspondence Extended Kalman Filter (EKF) to account for uncertainty present in the range images. For both the trials, the position estimates are then compared with those provided by ground truth to facilitate the performance evaluation of the registration algorithm. In addition,

we propose performance measures for assessing the quality of correspondences. These measures, collectively, provide an indication of the quality of the correspondences thus making the registration algorithm more robust to outliers as spurious matches are not used in computing the incremental transformation. The registration algorithm is then combined with proposed performance metrics and compared to the traditional ICP algorithm in terms of accuracy and speed.

The paper is structured as below: Section 2 describes the iterative temporal registration algorithm. Section 3 presents experimental results when the iterative algorithm is used for obtaining position estimates. Section 3.1 compares registration-aided position estimates with those provided by GPS. Section 3.2 details a map-aided registration algorithm for pose estimation. Section 4 develops performance measures for quality assessment of correspondences within the registration process and provides the associated results. Section 5 provides the conclusions and outlines areas of continuing research.

2. ITERATIVE TEMPORAL REGISTRATION ALGORITHM

The process of registration is stated formally as:

$$min_{(\mathbf{R},\mathbf{T})} \sum_i ||\mathbf{M}_i - (\mathbf{R}\mathbf{D}_i + \mathbf{T})||^2 \quad (1)$$

where $\mathbf{R}$ is the rotation matrix, $\mathbf{T}$ is the translation vector and the subscript i refers to the corresponding points of the sets $\mathbf{M}$ and $\mathbf{D}$.

2.1. Iterative Closest Point Algorithm

The ICP algorithm can be summarized as follows: Given an initial motion transformation between the two point sets, a set of correspondences are developed between data points in one set and the next. For each point in the first data set, find the point in the second that is closest to it under the current transformation. It should be noted that correspondences between the two point sets is initially unknown and that point correspondences provided by sets of closest points is a reasonable approximation to the true point correspondence. From the set of correspondences, an incremental motion can be computed facilitating further alignment of the data points in one set to the other. This find correspondence/compute motion process is iterated until a predetermined threshold termination condition.

In its simplest form, the ICP algorithm can be described by the following steps:

1. For each point in data set $\mathbf{D}$, compute its closest point in data set $\mathbf{M}$. In this paper, this is accomplished via nearest point search from the set comprising $N_{\mathbf{D}}$ data and $N_{\mathbf{M}}$ model points.
2. Compute the incremental transformation ($\mathbf{R}$,$\mathbf{T}$) using Singular Value Decomposition (SVD) via correspondences obtained in step **1.**
3. Apply the incremental transformation from step **2.** to $\mathbf{D}$.
4. If relative changes in $\mathbf{R}$ and $\mathbf{T}$ are less than a threshold, terminate. Else go to step **1.**

To deal with spurious points/false matches and to account for occlusions and outliers, we modify and weight the least-squares objective function in Equation (1) such that [11]:

$$min_{(\mathbf{R},\mathbf{T})} \sum_i w_i \ ||\mathbf{M}_i - (\mathbf{R}\mathbf{D}_i + \mathbf{T})||^2 \quad (2)$$

If the Euclidean distance between a point x_i in one set and its closest point y_i in the other, denoted by $d_i \triangleq d(x_i, y_i)$, is bigger than the maximum tolerable distance threshold $\mathcal{D}_{max}$, then w_i is set to zero in Equation (2). This means that an x_i cannot be paired with a y_i since the distance between reasonable pairs cannot be very big. The value of $\mathcal{D}_{max}$ is set adaptively in a robust manner by analyzing distance statistics.

Let $\{x_i, y_i, d_i\}$ be the set of original points, the set of closest points and their distances, respectively. The mean and standard deviation of the distances are computed as:

$$\mu = \frac{1}{N}\sum_{i=1}^{N} d_i; \quad \sigma = \sqrt{\frac{1}{N}\sum_{i=1}^{N}(d_i - \mu)^2}$$

where N is the total number of pairs.

The pseudo-code for the *Adaptive Thresholding* (AT) of the distance $\mathcal{D}_{max}$ is given below:

$$\begin{array}{c} \texttt{if } \mu < \mathcal{D} \\ \mathcal{D}^{itn}{}_{max} = \mu + 3\sigma\texttt{;} \\ \texttt{elseif } \mu < 3\mathcal{D} \\ \mathcal{D}^{itn}{}_{max} = \mu + 2\sigma\texttt{;} \\ \texttt{elseif } \mu < 6\mathcal{D} \\ \mathcal{D}^{itn}{}_{max} = \mu + \sigma\texttt{;} \\ \texttt{else } \mathcal{D}^{itn}{}_{max} = \epsilon\texttt{;} \end{array}$$

where itn denotes the iteration number and $\mathcal{D}$ is a function of the resolution of the range data.

During implementation, $\mathcal{D}$ was selected based on the following two observations:

1) If $\mathcal{D}$ is too small, then several iterations are required for the algorithm to converge and several good matches will be discarded, and
2) If $\mathcal{D}$ is too big, then the algorithm may not converge at all since many spurious matches will be included. The interested reader is referred to [11] for more details on the effect and selection of $\mathcal{D}$ and ϵ on the convergence of the algorithm.

At the end of this step, two corresponding point sets, $\mathbf{P_M}$:$\{\mathbf{p}_i\}$ and $\mathbf{P_D}$:$\{\mathbf{q}_i\}$ are available.

The incremental transformation (rotation and translation) of step **2.** is obtained as follows:

- Calculate $\mathbf{H}$=$\sum_{i=1}^{N_D}(\mathbf{p}_i - \mathbf{p}_c)(\mathbf{q}_i - \mathbf{q}_c)^T$; ($\mathbf{p}_c$,$\mathbf{q}_c$) are the centroids of the point sets ($\mathbf{P_M}$,$\mathbf{P_D}$).

- Find the Singular Value Decomposition (SVD) of $\mathbf{H}$ such that $\mathbf{H} = \mathbf{U}\mathbf{\Omega}\mathbf{V}^T$ where $\mathbf{U}$ and $\mathbf{V}$ are unitary matrices whose columns are the singular vectors and $\mathbf{\Omega}$ is a diagonal matrix containing the singular values.
- The rotation matrix relating the two point sets is given by $\mathbf{R} = \mathbf{V}\mathbf{U}^T$.
- The translation between the two point sets is given by $\mathbf{T} = \mathbf{q}_c - \mathbf{R}\mathbf{p}_c$.

This process is iterated as stated in step **4.** until the mean Euclidean distance between the corresponding point sets $\mathbf{P_M}$ and $\mathbf{P_D}$ is less than or equal to a predetermined distance or until a given number of iterations is exceeded.

3. EXPERIMENTAL RESULTS

3.1. Registration-aided Position Estimation

In this section, we estimate the position of an UGV operating in an unknown outdoor environment. The registration algorithm is used for aiding position estimation whenever GPS errors are above a predetermined threshold[1].

An Extended Kalman Filter (EKF) was used to fuse encoder, GPS and compass observations to arrive at *ground truth* position estimates. It should be noted here that the EKF pose estimate is always superior than that provided by GPS alone and thus has been considered as ground truth. Consequently, a better position fix is guaranteed even when GPS is subject to multipathing errors. The ground truth was obtained in a similar fashion as reported in [8].

Figure 1 shows the results of the position estimation using the registration algorithm. As mentioned earlier, registration of range images is used to aid position estimation when GPS reported positional errors exceed a given threshold. In Figure 1(a), the registration-aided position estimates are denoted by '$+$' and that of the GPS by '$\circ$'. The wheel encoder estimates are also shown by '$\times$' for comparison. The error between the GPS and the registration-aided position estimates as compared with the ground truth are shown in Figure 1(b). It is evident that the registration-aided estimates are far superior than that of GPS alone.

3.2. 2D Map-aided Position Estimation

A map-aided position estimation algorithm for computing accurate pose estimates for a UGV operating in tunnel-like environments is described in this section. Using ground truth[2] together with the information from a range and bearing scanning laser rangefinder, a map of the operating domain, represented by a polyline that adequately approximates the geometry of the environment, is obtained. The map building process relies on position estimation provided by artificial landmarks.

An Iterative Closest Point-Extended Kalman Filter (ICP-EKF) algorithm is used to match range images from a scanning laser rangefinder to the line segments of the polyline map [6]. For this application, ICP alone does not provide sufficiently reliable and accurate vehicle motion estimates. These shortcomings are overcome by combining the ICP with a post-correspondence EKF. Once correspondences are established, a post-correspondence EKF, with the aid of a non-linear observation model, provides consistent vehicle pose estimates.

The ICP-EKF algorithm has several advantages. First, the uncertainty associated with observations is explicitly taken into account. Second, observations from a variety of different sensors can be easily combined as the changes are reflected only as additional observational states in the EKF. Third, laser observations that do not correspond to any line segment of the polyline map are discarded during the EKF update stage thus making the algorithm robust to errors in the map.

The estimated vehicle positions (solid line)[3] provided by the ICP-EKF algorithm along with the ground truth (dotted line) is shown in Figure 2(a). The vehicle travels a distance of 150 meters from right to left. The corresponding 2σ confidence bounds for the absolute error in x, y and ϕ are shown in Figure 2(b). It can be seen that the errors are bounded and thus the pose estimates are consistent. It is also clear that the estimated path is in close agreement with the ground truth.

4. PERFORMANCE MEASURES

The correspondence determination process is the most challenging step of the iterative algorithm. Establishing reliable correspondences is extremely difficult as the UGV is subjected to heavy pitching and rolling motion characteristic of travel over undulating terrain. This is further exacerbated by the uncertainty of the location of the sensor platform relative to the global frame of reference. In addition to these factors, noise inherently present in range images complicates the process of determining reliable correspondences.

One solution to overcome the above deficiencies is to extract naturally occurring view-invariant features, for example, corners, from range images. Such *ground control points* can then be used for establishing reliable registration with the ICP algorithm converging to the global minimum. A hybrid approach to register aerial images obtained from a UAV with those from the UGV was developed by augmenting the modified ICP algorithm with a feature-based method. The feature-based hybrid approach was shown to be effective in producing reliable registration for UGV navigation [9].

For the map-aided position estimation scheme described in Section 3.2, the ICP-EKF algorithm failed to produce

[1]The error in the GPS positions reported were obtained as a function of the number of satellites acquired. As an alternative, the so-called *dilution of precision* measure associated with the GPS can be used for the same purpose [2].

[2]The ground truth was obtained using a rotating laser scanner and known artificial landmarks placed at surveyed locations [7].

[3]As the estimates and the their corresponding ground truth are very close, extra effort is required on the part of the reader to distinguish between the two.

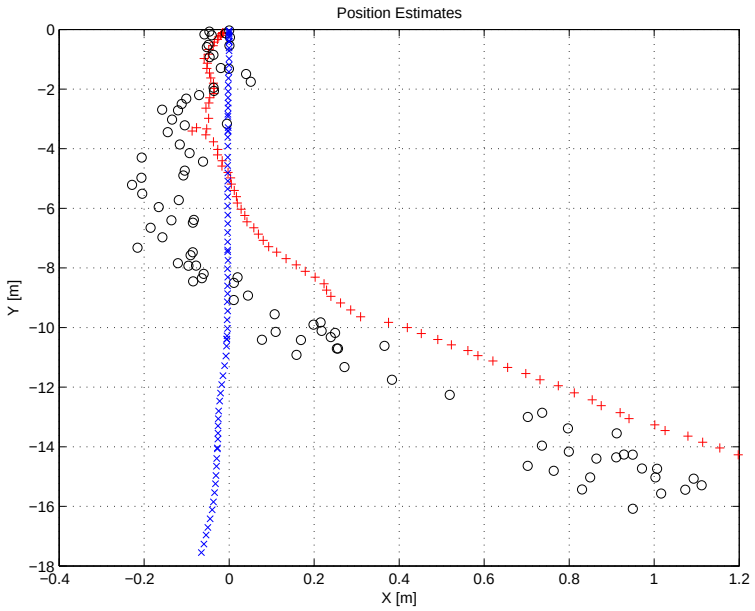

(a)

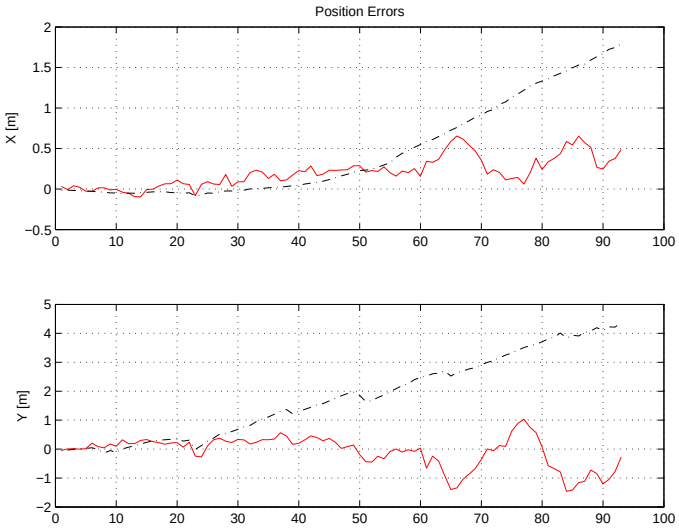

(b)

Fig. 1. Registration-aided position estimation. The aided estimates are shown by '+' and that of GPS by 'o'. The wheel encoder estimates shown by '×' are included for comparison. In (b), position errors as compared to the ground truth is depicted (GPS estimate is shown in dashed-dotted line).

unambiguous correspondences with the map whenever variations in data sets were not unique. To enable ICP to produce accurate correspondences, a strategy to augment the ICP-EKF algorithm with artificial/natural landmarks was devised to provide external aiding. To facilitate the selection of landmarks, an entropy-based metric was developed to enable the evaluation of information contained in a potential landmark. A curvature scale space algorithm was developed to extract natural landmarks from laser rangefinder scans [5]. The proposed landmark augmentation methodology has been verified for the localization of a Load-Haul-Dump truck and resulted in the ICP-EKF algorithm producing reliable and consistent estimates [6].

We propose the following measures towards performance evaluation of the registration algorithm for position estimation.

4.1. ICP Estimate and Dead-reckoning Prediction Measure

The ICP itself can be used to compute the estimates of the pose of the UGV. This can be compared with dead-

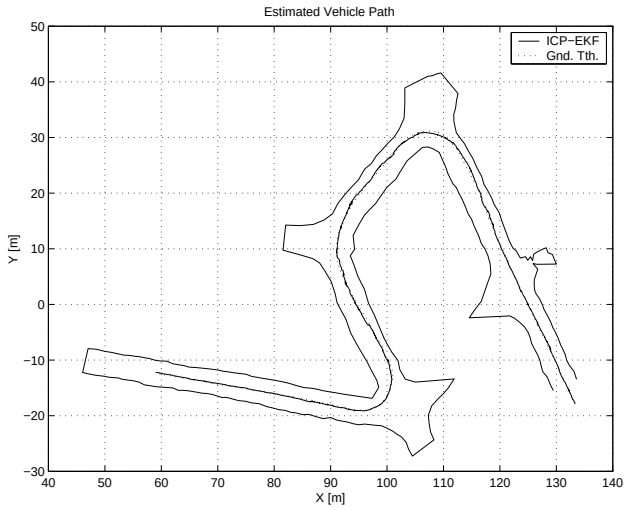

(a)

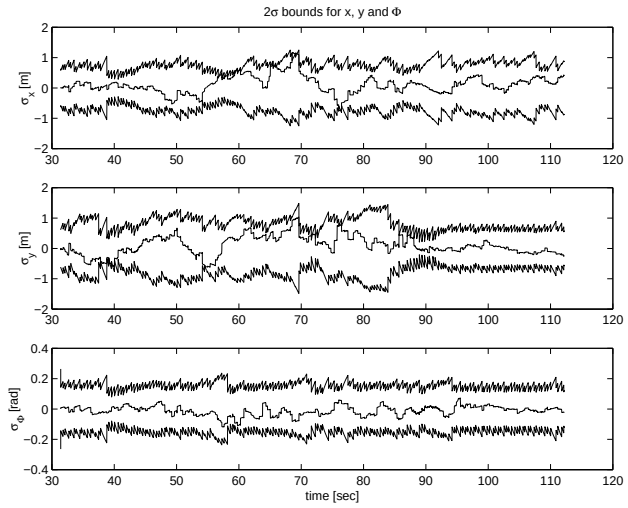

(b)

Fig. 2. 2D Map-aided Position Estimation. ICP-EKF estimated position the trial vehicle (solid line) and the ground truth (dotted line) are shown in (a). The 2σ confidence bounds are computed using the covariance estimate for the error in x, y and ϕ compared to the actual error computed with the ground truth estimates as depicted in (b).

reckoning estimates each time before the correspondences are computed. More specifically, the prediction covariance (from dead-reckoning) can be utilized as a check on the ICP estimates, since if the associated state covariances become large, this is an indication of the state estimation filter divergence as a result of the poor ICP estimates.

The largest Eigen value of the predicted state covariance matrix (that is a measure of the total positional uncertainty) can be used as a measure to check the quality of the ICP estimates.

Also the determinant of the predicted state covariance matrix can be used as a measure since it represents total predicted uncertainty and this can be observed to see if the ICP produces reliable and non-divergent estimates (since once the ICP estimates start behaving erratically, this is reflected by similar behavior in the correspondences).

4.2. Mean Squared Error Measure

To indicate if the correspondences make sense the following measure is proposed:

$$\mathcal{P}_{mse} \quad = \quad \frac{1}{n}\sum_{i=1}^{n}\left[d\left(p_i,\ell_i\right)\right]^2$$

where p_i and ℓ_i are the i^{th} of n range data points and $d\left(p_i,\ell_i\right)$ is the distance from the p_i^{th} point to the ℓ_i^{th} point. Global minimum of the function will occur at the *true* pose of the vehicle.

At the true pose, all or at least the majority of the range data points will be close to their corresponding points, thus yielding a very low value for the correct solution. The problem with this measure is that it is difficult to decide if the pose is true in the presence of outliers and occlusions.

4.3. Classification Factor

Similar to [4], we define *well defined data points* as those points that lie within some distance threshold from their corresponding points:

$$\mathcal{P}_{cf} \quad = \quad \frac{1}{n}\sum_{i=1}^{n}\left(1-\frac{d^m}{d^m+c^m}\right)$$

where d = d(p_i,ℓ_i), c = neighborhood size, m = sigmoid steepness[4]. At true pose, global maximum should approach close to unity and will be less in the neighborhood of well defined data points. Note that $\mathcal{P}_{cf}$ values can fall only between [0,1].

Indirectly this measure indicates the *future-goodness* of the pose estimate if a certain threshold is exceeded. The problem with this measure could be that it is not as sensitive as $\mathcal{P}_{mse}$ since it applies only for a certain local neighborhood. Thus $\mathcal{P}_{mse}$ can be used as a comparative performance measure whereas $\mathcal{P}_{cf}$ for pass/fail decisions for the correspondences before they are passed on for computing the incremental transformation.

4.4. Comparative Performance Measure

It is the ratio defined by

$$\mathcal{P}_{cpm} \quad = \quad \frac{{\mathcal{P}_{cf}}^2}{\mathcal{P}_{mse}}$$

The peak of this measure should occur at the true pose. In other words, this measure serves as a nonlinear scaling factor applied to the inverse of the measure, $\mathcal{P}_{mse}$.

[4]A sigmoid function is given by $f(a) = \frac{1}{1+e^{-ga}}$ where g denotes gain.

4.5. Results and Discussion

In this section, we use 3D LADAR data obtained during field trials to illustrate the utility of the proposed metrics in assessing the quality of correspondences. The LADAR was mounted on a UGV traversing rugged terrain on a pan/tilt platform to increase its narrow 20° field of view. The range of the tilt motion is $\pm 30^\circ$ resulting in an effective field of view of about 90° and providing a range image of 32 lines $\times$ 180 pixels where each data point contains the distance to a target in the operating environment. The angular resolution of this LADAR is $0.658^\circ \times 0.5^\circ$ in the horizontal and vertical directions, respectively.

We illustrate the combined utility of adaptive thresholding and the $\mathcal{P}_{mse}$ measure by using it to register 3D range images. We then compare the registration results with direct ICP (i.e., without AT and $\mathcal{P}_{mse}$). For the comparison, the same termination threshold condition is employed for both the algorithms.

Figures 3 and 4 summarize the comparative results. Figures 3(a) and (b) show the registered LADAR images via the direct and combined ICP algorithms, respectively. The combined ICP needed 39 iterations whereas the direct ICP took 82 iterations. The mean distances before and after registration were 0.19 m and 0.07 m for the two algorithms, respectively. Figures 4(a) and (b) show the closest point distance before and after registration. It is thus evident that the combined ICP algorithm is vastly superior than the direct ICP algorithm both in terms of accuracy and speed. Even though the $\mathcal{P}_{mse}$ metric is sensitive to outliers, we contend that the adaptive thresholding methodology in combination with the mean-squared error metric provides an acceptable means in inferring the validity of the position estimate.

5. CONCLUSIONS AND FURTHER WORK

The evaluation of performance of an iterative registration algorithm for position estimation of UGVs operating in unstructured environments was the main theme of this paper. The modified ICP algorithm was used to aid the position estimation process and the resulting estimates were compared with ground truth to facilitate the performance evaluation for two sets of field data. Field data obtained from trials on UGVs traversing undulating outdoor terrain was used to quantify the performance of the algorithm in producing continual position estimates.

In the first set of experimental results, registration-aided position estimates were generated whenever GPS estimates were unavailable or unreliable. For the second set of trials, the ICP-EKF algorithm was used for map-aided position estimation. In both cases, the presented results demonstrated the efficacy of the registration algorithm for position estimation.

The second part of the paper developed performance measures towards assessing the quality of correspondences required for accurate and efficient registration. The modified algorithm was combined with the mean-squared error metric to register 3D LADAR range images. The combined algorithm was then evaluated against the direct ICP algorithm. The accompanying results showed the superiority of the combined algorithm both in terms of speed and accuracy.

Future work includes combining the measures to achieve efficient 3D registration for mapping and position estimation tasks, both in indoor and outdoor environments. Currently, we are in the process of obtaining LADAR data in areas where GPS accuracy degrades and then approaches its best estimate. Such data sets would be of immense value in evaluating the utility of the registration algorithm and the proposed performance measures.

6. REFERENCES

[1] P. Besl and N. McKay. A Method for Registration of 3-D Shapes. *IEEE Transactions on Pattern Analysis and Machine Intelligence*, 14(2):239–256, 1992.

[2] M.S. Grewal, L.R. Weill, and A.P. Andrews. *Global Positioning Systems, Inertial Navigation and Integration*. Wiley, 2001.

[3] I. Kweon and T. Kanade. High Resolution Terrain Map from Multiple Sensor Data. In *Proceedings of the IEEE International Workshop on Intelligent Robots and Systems*, volume 1, pages 127–134, 1990.

[4] P. MacKenzie and G. Dudek. Precise Positioning using Model-based Maps. In *Proceedings of the IEEE International Conference on Robotics and Automation*, pages 1615–1621, 1994.

[5] R. Madhavan and H. Durrant-Whyte. Natural Landmark-based Autonomous Navigation using Curvature Scale Space. *Robotics and Autonomous Systems*, 46(2):79–95, February 2004.

[6] R. Madhavan and H. Durrant-Whyte. Terrain Aided Localization of Autonomous Ground Vehicles. *Special Issue of the Journal of Automation in Construction (Invited)*, 13(1):69–86, January 2004.

[7] R. Madhavan et al. Evaluation of Internal Navigation Sensor Suites for Underground Mining Vehicle Navigation. In *Proceedings of the IEEE International Conference on Robotics and Automation*, pages 999–1004, May 1999.

[8] R. Madhavan, K. Fregene, and L.E. Parker. Distributed Cooperative Outdoor Multi-robot Localization and Mapping. *Autonomous Robots: Special Issue on Analysis and Experiments in Distributed Multi-Robot Systems*, 17(1):23–39, July 2004.

[9] R. Madhavan, T. Hong, and E. Messina. Temporal Range Registration for Unmanned Ground and Aerial Vehicles. In *Proceedings of the IEEE International Conference on Robotics and Automation*, pages 3180–3187, April 2004.

[10] G. Shaffer. *Two-Dimensional Mapping of Expansive Unknown Areas*. PhD thesis, Carnegie Mellon University, 1992.

[11] Z. Zhang. Iterative Point Matching for Registration of Free-Form Curves and Surfaces. *International Journal of Computer Vision*, 13(2):119–152, 1994.

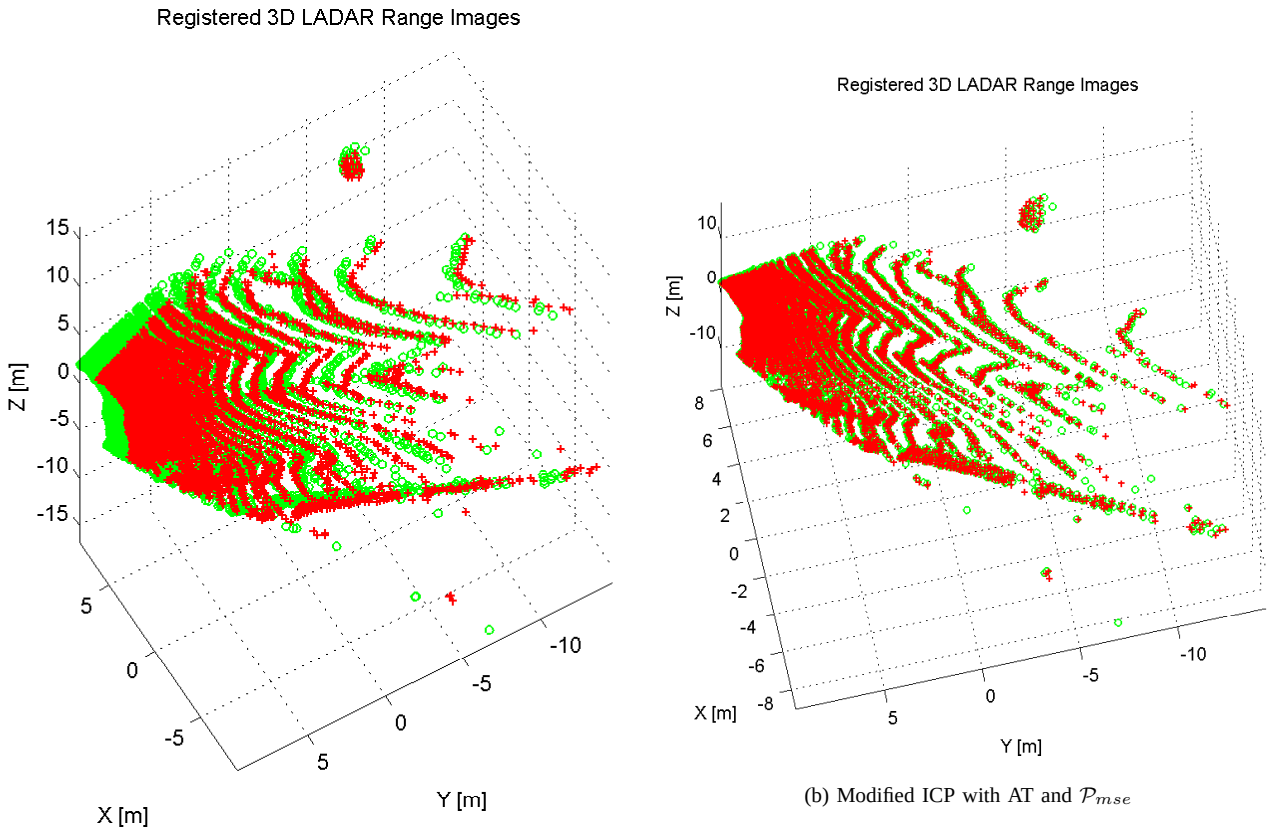

(a) Direct ICP

(b) Modified ICP with AT and $\mathcal{P}_{mse}$

Fig. 3. Illustration of 3D LADAR registration via the direct (w/o AT and $\mathcal{P}_{mse}$) and combined ICP algorithms. The model ('$\circ$') and data ('+') points after registration are shown.

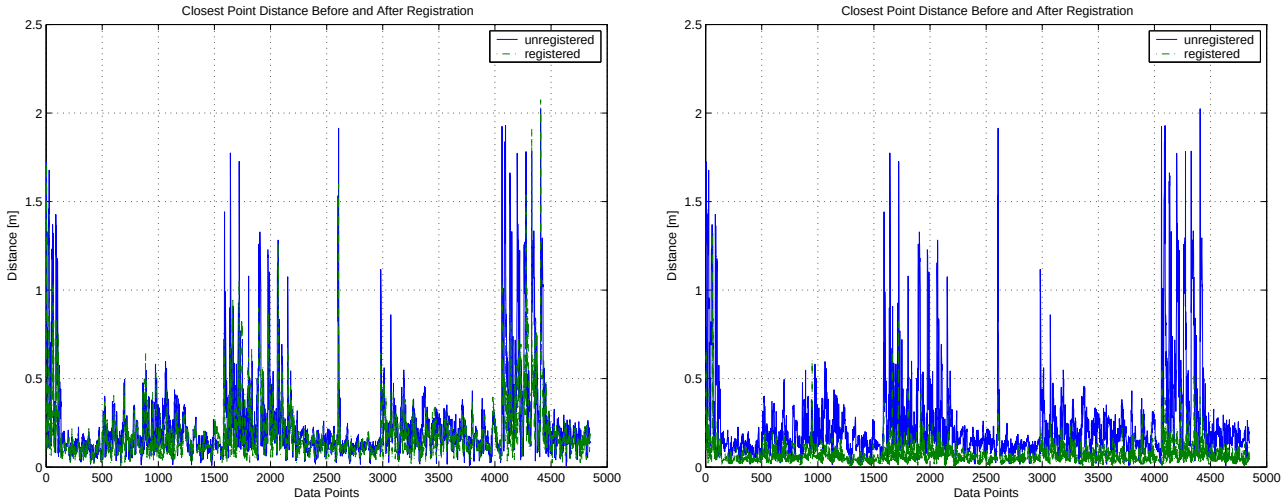

(a)

(b)

Fig. 4. The registered (shown in dashed-dotted line) and unregistered closest point distances are shown corresponding to the registration of range images depicted in Figures 3(a) and 3(b), respectively.